Crystal Structures and Melting Points of Saturated Triacylglycerols in the β-3 Phase

T.C. van Soest, S. de Jong* and **E.C. Roijers**
Unilever Research Laboratorium Vlaardingen, P.O. Box 114, Vlaardingen, The Netherlands

A comprehensive packing analysis is presented of the crystal structures of a large number of saturated triacylglycerols in the β-3 phase. The triacylglycerols *p.q.r* have been grouped into four classes: *r=p*, *p+2*, *p+4* and *p+6*. The length of the middle chain, *q*, dictates whether a β-2 or β-3 packing occurs. The latter packing arrangement is adopted when *q* differs at least 4 from *p* or *r*.

The model-building approach starts from the known molecular conformation of β-2 *10.10.10* and the $T_{//}$ subcell packing mode of the hydrocarbon chains. Purely geometrical model-building allows a preliminary assignment of crystal structures. Crystal lattice energy calculations using the atom-atom potential method support these tentative assignments and clarify some details regarding the stacking of layers. In common with the β-2 phase crystal structures, the structure of the terrace-like arrangement of the terminal methyl groups plays a crucial role. Triacylglycerols with chains 1 and 3 differing 2 or 4 carbon atoms have a common arrangement of the end-methyl groups (type β-3*A*). Those with a difference of 0 (i.e. symmetrical) or 6 carbon atoms have a different, less favorable methyl terrace (type β-3*B*). The available experimental evidence (x-ray powder diffraction, unit-cell data and melting points) is entirely compatible with these proposals.

The growth of good single crystals of acylglycerols is beset with extremely great difficulties. A complete solution of the crystal structure is hard to obtain, even if single crystals are available. There is therefore a need for alternative approaches toward the solution of acylglycerol crystal structures.

For an up-to-date review of crystal structure analyses of lipid systems see (1) and (2); for a more general treatment of the polymorphism of fatty systems see (3) and (4).

In a previous study (5) we derived detailed packing modes of a large number of saturated triacylglycerols in the β-2 phase, extrapolating from one known crystal structure by using a model-building approach. Particularly important features of this approach were the systematic packing of the hydrocarbon chains ($T_{//}$ subcell) and the terrace-like structure of the end methyl groups at the layer boundaries. For each triacylglycerol, two or three distinct solutions could be advanced, only one of which, in general, was compatible with powder diffraction and melting-point data. In the present work, a similar approach is applied to the β-3 phase of triacylglycerols.

Roughly, the β-3 phase is observed for those triacylglycerols having a middle chain which differs considerably in length from (one of) the outer chains. This renders the β-2 packing, with chains 1, 2 and 3 packed adjacent in the crystal lattice, less favorable as compared to the β-3 packing mode where the chains are more or less sorted by their lengths (Fig. 1). This was first realized by Lutton (6), who could thus satisfactorily account for the larger long spacings.

Table 1 summarizes experimental long-spacing and melting-point values reported for β-3 phase triacylglycerols *p.q.r* with saturated fatty acid chains. The criteria for designating a particular crystalline phase as β-3 are the presence of the characteristic β-type short spacings (strong lines near 0.46 and 0.38 nm) and a long spacing which is about 1.5 times larger than could be expected for a β-2 phase crystal structure. The triacylglycerols *p.q.r* in Table 1 have been grouped into four classes: *r=p*, *p+2*, *p+4* and *p+6*. It appears that *q* always differs by four or more from *p* and/or *r*.

Contrary to our previous work on the β-2 phase, we cannot benefit from a completely solved β-3 phase crystal structure which might serve as a starting point for other β-3 triacylglycerols. Thus we are forced to transfer some features of the β-2 crystal structures to the β-3 phase, and to proceed with the model building using general packing principles. All this has to be done within the constraints imposed by the experimental data of Table 1.

Geometric packing analysis—molecular geometry. A vital assumption in our analysis concerns the molecular geometry. It is conceivable that the molecular geometry in the β-3 phase differs from that in the β-2 phase. In that case, one cannot proceed with the packing analysis since it is hard to tell what the different geometry would look like in detail. On the other hand,

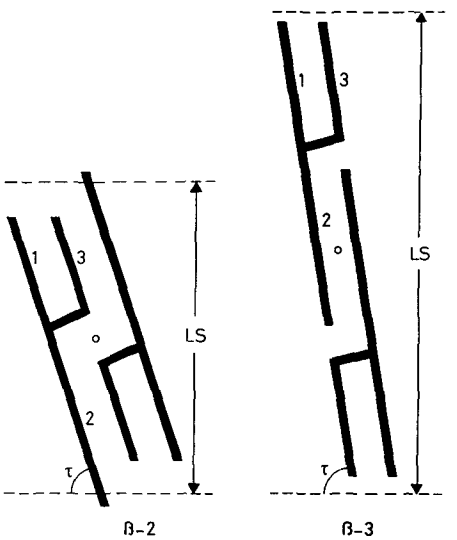

FIG. 1. Arrangement of triacylglycerol molecules in the β-2 and β-3 modifications.

*To whom correspondence should be addressed.

TABLE 1

Experimental Long-Spacing (L) and Melting-Point (T_m) Data of β-3 Phase Triacylglycerols with Saturated Acyl Chains

	p.q.r	*n*	*L*/nm	(Refs.)	T_m/°C	(Refs.)
	10.14.10	34	4.65	(7)	34.0	(7)
	10.16.10	36	4.95	(7)	40.0	(7)
	10.18.10	38	5.16	(7)	44.5,45.0	(7,8)
	14.10.14	38	5.25	(7)	43.0	(7)
	16. 6.16	38	5.25	(9)	44.5,45.8	(9,10)
	12.18.12	42	5.68	(7)	47.0,51.5,50.9	(7,8,11)
p.q.p	*16.10.16*	42	5.65	(7)	51.5,52.0	(7,10)
	18. 6.18	42	5.68	(9)	53.1,53.0	(9,12)
	16.12.16	44	5.90	(7)	53.5,54.6,55.0	(7,10,13)
	18.10.18	46	6.12,5.86	(7,1)	57.0,56.5,58.2	(7,1,12)
	18.12.18	48	6.37	(7)	60.5,60.5,59.8	(7,12,14)
	18.14.18	50	6.58,6.63	(7,15)	62.5,63.0,63.8	(7,12,15)
	16.22.16	54	7.04	(16)	66.6	(16)
	18.22.18	58	7.51	(16)	70.6	(16)
	16.10.18	44	6.00	(17)	55.0,53.5	(17,18)
p.q.p+2	*16.12.18*	46	6.12	(17)	57.5,56.5	(17,18)
	16.14.18	48	6.34	(17)	59.5,59.7	(17,19)
	10.10.14	34	4.75	(20)	34.5	(20)
	12.12.16	40	5.46	(20)	46.5,47.5	(20,21)
p.q.p+4	*14.10.18*	42	5.73	(17)	52.5,51.0	(17,18)
	14.12.18	44	5.98	(17)	55.0	(17)
	14.14.18	46	6.14,6.17	(20,22)	56.0,57.0,56.4	(20,22,23)
	18.18.22	58	7.55	(22)	70.7	(22)
	10.10.16	36	4.97	(20)	35.0	(20)
	12.10.18	40	5.49	(17)	41.8	(17)
p.q.p+6	*10.16.16*	42	5.62	(20)	45.5	(20)
	12.12.18	42	5.70,5.72	(20,6)	45.0,44.5,45.4	(6,10,20)
	12.14.18	44	5.96	(17)	49.5	(17)
	12.16.18	46	6.24	(17)	52.0	(17)

one may well argue that a different packing (β-3 vs β-2) does not bring about any major changes in molecular conformation. Strong evidence, although no proof, for the correctness of this assumption is obtained if the packing analysis can be completed successfully.

Therefore, just as in our earlier β-2 analysis, the molecular geometry of a triacylglycerol *p.q.r* is obtained by adopting the molecular structure of β-2 *10.10.10* (24) and by adjusting the chain lengths. In fact, for the subsequent analysis, slight alterations in the geometry at the glycerol group are allowed, as long as these do not affect the relative positions of the three hydrocarbon chains: chains 1 and 3 run parallel (already packed according to the $T_{//}$ subcell), whereas chain 2 runs in exactly the opposite direction. For asymmetric triacylglycerols *(p≠r)*, we assume that the longer of the two equivalent outer chains takes position 3 and the shorter takes position 1, just as in the β-2 phase (Fig. 1).

Molecular pairs. The structure of the molecular pair constitutes the main difference with the β-2 packing mode. Chains 2 are now packed side by side in the center of the molecular bilayer, with chains 1 and 3 at both outer sides. In principle, four different symmetric arrangements are conceivable (Fig. 2).

Only the first case *(i)* can be reconciled simply with the $T_{//}$ subcell packing mode, which has $P\bar{1}$ symmetry. The other symmetries are virtually incompatible with a $T_{//}$ hydrocarbon chain packing. Apart from this, case *(iv)* would lead to an angle of tilt $\tau = 90°$, in contrast to the observed value of about 66°. Furthermore, cases *(ii)* and *(iii)* give rise to molecular layers built up from a single stereoisomer. For the racemic asymmetric triacylglycerols *(p≠r)*, a segregation of molecules of opposite chirality in separate layers must be envisaged, which is not likely from the point of view of crystal-growth mechanism. In view of all these considerations, symmetries *(ii)*, *(iii)* and *(iv)* have been ruled out.

For the sake of completeness a fifth alternative "symmetry" should be mentioned as well: no symmetry at all. It implies different conformations for the two molecules forming the pair, and places no restriction on their packing arrangement: two factors which greatly complicate a packing analysis. The no-symmetry alternative is, however, unlikely from the outset, as the occurrence of two independent molecules in the crystallographic unit cell is a fairly rare phenomenon. Even then, it is not uncommon that there are only small local deviations from symmetry. In that case, a symmetric solution is useful since it serves as a good approximation to the exact structure.

We will pursue our packing analysis assuming packing around a center of symmetry. The packing may be specified more accurately by requiring that carbon chains 2 are related by a subcell $\mathbf{a}_s$ translation. Starting from a molecular pair (Fig. 1) in the β-2 packing mode, the β-3 type packing is obtained by a shift **d** of one of the molecules such that chain 2 takes the posi-

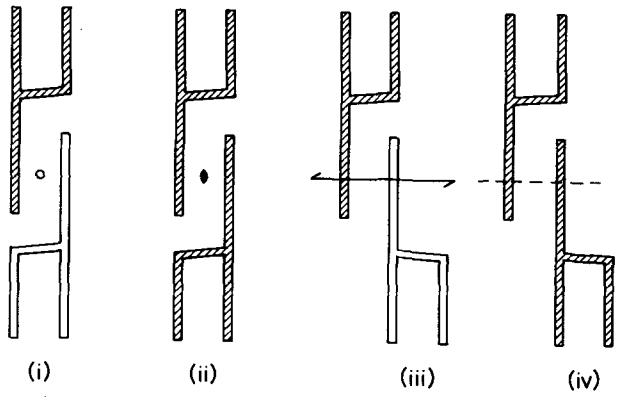

FIG. 2. The four different packing modes of a pair of triacylglycerol molecules in the β-3 phase: *(i)* a center of symmetry; *(ii)* a twofold rotation axis normal to the molecular plane; *(iii)* a twofold screw axis lying in the molecular plane at right angles to the chain axes; and *(iv)* a glide plane perpendicular to the chain axes. The open and hatched models distinguish between the two sides of the molecule.

tion that chain 3 has left. Expressing the shift **d** in terms of subcell axes we find:

$$\mathbf{d} = 1.12\,\mathbf{a}_s - 0.01\,\mathbf{b}_s + (q/2+0.83)\,\mathbf{c}_s \qquad [1]$$

A subsequent shift of one of the molecules towards the other over one $\mathbf{c}_s$ subcell period would also satisfy the $T_{/\!/}$ subcell packing condition, but it would create short intermolecular contacts (viz. C•••C 0.19, C•••H 0.13, O•••H 0.19, H•••H 0.09 nm).

a-*Axis packing.* Completely analogous to the β-2 packing analysis (5), the molecular pairs are now placed in a lateral fashion giving a "one-dimensional" crystal with the unit-cell **a** axis. The $T_{/\!/}$ subcell packing dictates the following expression for this axis:

$$\mathbf{a} = 2\mathbf{a}_s + t\mathbf{c}_s\ (t=0, \pm1, \pm2, \ldots) \qquad [2]$$

Using the molecular geometry and the subcell dimensions of β-2 *10.10.10* (24), we have verified that no short contacts arise for $t = -4,\ldots, 4$ using atomic radii of 0.15 nm for C, 0.13 nm for O and 0.10 nm for H. Such small radii (about 0.02 nm shorter than the normal van der Waals radii) have been used in order not to eliminate a packing possibility too easily.

As in Reference 5, attention is called to the structure of the methyl-group boundary, which now consists of only two methyl-to-methyl steps for each *a* period, connecting the methyl groups of chains 1 of neighboring unit cells via the methyl carbon of chain 3 (Fig. 3).

The following relations between the **a** axis, the methyl-to-methyl steps $\mathbf{a}_1$ and $\mathbf{a}_2$, and the lengths of chains 1 and 3 apply:

$$\mathbf{a} = \mathbf{a}_1 + \mathbf{a}_2, \qquad [3]$$

$$\mathbf{a}_i = \mathbf{a}_i + t_i\mathbf{c}_s \quad (i = 1,2), \qquad [4]$$

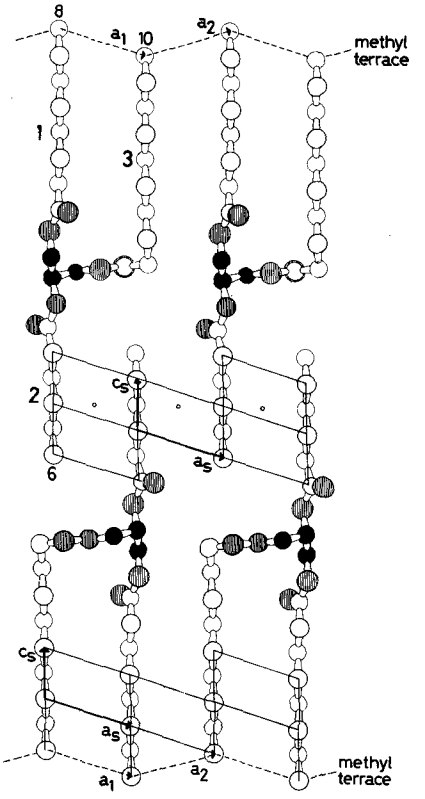

FIG. 3. Packing of the molecular pairs in the *a* direction showing the arrangement of a pair of molecules around their center of symmetry and the structure of the (0,1)-terrace for a *p.q.p*+2 triacylglycerol *(8.6.10).*

$$t = t_1 + t_2, \qquad [5]$$

where

$$t_1 = (r - p - 2)/2 \qquad [6.1]$$

and

$$t_2 = 0, \pm1, \pm2, \ldots \qquad [6.2]$$

The methyl boundary can be designated by a set of two boundary indices (t_1,t_2). A triacylglycerol with t_1=i and a triacylglycerol with t_1=j (≠i) can, in principle, pack in the same β-3 submodification having the . . .ijijiji. . . methyl terrace. Hence, in the β-3 phase, each terrace is associated with two different sets of homologous series of triacylglycerols, each set being characterized by a common value for *(r-p)*. The length of chain 2, *q*, is quite immaterial for the packing.

b-*Axis packing.* The packing in the **b** direction must again conform to the subcell packing, giving:

$$\mathbf{b} = u\mathbf{a}_s + \mathbf{b}_s + v\mathbf{c}_s \quad (u=0,1;\ v=0,1,2,\ldots.) \qquad [7]$$

An examination of all possibilities showed that very short contacts (<0.155 nm) were present for all cases, except for $u = v = 0$. Thus, just as for the β-2 modification, we have:

$$\mathbf{b} = \mathbf{b}_s \qquad [8]$$

Contact calculations for an entire molecular layer, extending in both the **a** and **b** direction, revealed that there are some short contacts between molecules along the [110] direction. Figure 4 shows, for several values of t, the shortest contacts for some types of atom-atom interaction occurring in the two-dimensional crystal defined by the **a** axis and **b** axis of Equations 2 and 8, respectively.

There is a clear preference for $t = -1$ or $+1$, in contrast to $t = 0$. It should be borne in mind, however, that the calculations have been based on the geometry of β-2 *10.10.10*. The short contacts mostly involve atoms at the glycerol group and we may not completely rule out the possibility that these contacts are removed by some adaptation of the molecular conformation to the different crystal packing.

The relation between the unit cell and the subcell may also be given by the subcell Miller indices of the *ab* plane (25). For the β-3 phase, the hydrocarbon chain packing may thus be characterized as $T_{//}$ $(t0\bar{2})$. The angle of tilt τ, i.e. the angle between the chain axes and their projection on the *ab* plane, can then be calculated as:

$$\tau = \arcsin\left[2(d_{t0\bar{2}})_s/c_s\right] \qquad [9]$$

Using the same dimensions for the $T_{//}$ subcell as before (1), we find $\tau = 56.0°$, 67.4°, 70.0° and 60.1° for $t = -1$, 0, 1 and 2, respectively. Since the experimental value for τ (calculated from the slope of the long-spacing line plotted as a function of n) is about 66°, it is clear that especially $t = 0$ and $t = 1$ packings need be considered further.

c-Axis packing. Generally the layers may be stacked around one of the following three symmetry elements: *(i)* a center of symmetry, *(ii)* a (glide) mirror plane, or *(iii)* a twofold (screw) axis. Each of these possibilities will be discussed in turn.

(i) This case corresponds to a straightforward stacking of the layers without introducing any new symmetry elements. The space group becomes $P\bar{1}$, just as for the β-2 phase. Unlike the β-2 form, however, the layer stacking now imposes no restrictions on the boundary indices. The precise *c*-axis packing can be derived quite easily, starting from a triacylglycerol in the β-2 type-*D* crystal structure ($t_1 = t_2 = t_3 = 0$) with the **c** axis described by Equations 8 and 9.2 of Reference 5. By combining this β-2*D* **c** axis with the shift **d** necessary to transform the β-2 into the β-3 packing mode (Eq. 1) we obtain the following β-3 **c** axis:

$$\mathbf{c} = (0.43-1+1.12)\mathbf{a}_s + (0.51-0.01)\mathbf{b}_s + \left(3.54+\frac{p+r-2+q}{2}+0.83\right)\mathbf{c}_s$$

or in short:

$$\mathbf{c} = \mathbf{c}_o + 1/2\, n\mathbf{c}_s, \qquad [10]$$

where

$$\mathbf{c}_o \equiv 0.55\mathbf{a}_s + 0.50\mathbf{b}_s + 3.38\mathbf{c}_s \qquad [11]$$

and

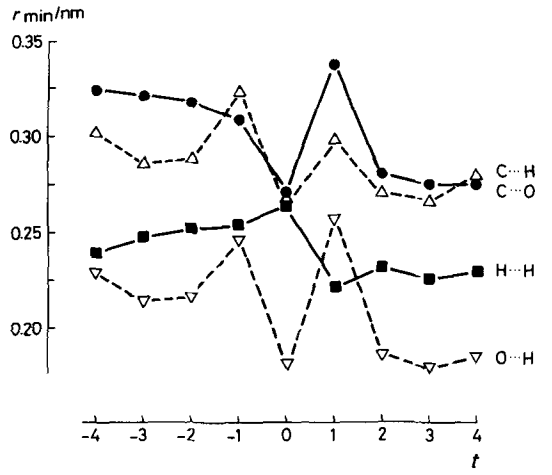

FIG. 4. Shortest intermolecular atom-atom distances (r_{min}) for different choices of the *a* axis ($=2\mathbf{a}_s+t\mathbf{c}_s$). (△)C•••H; (●)C•••O; (■)H•••H; (▽)O•••H.

$$n \equiv p + q + r \qquad [12]$$

The above expression for $\mathbf{c}_o$ has been derived for the case $t=0$. To include other terraces as well, ($t \neq 0$), Equation 11 must be slightly generalized in order to make the unit-cell volumes independent of the terrace structure, just as we demanded of the β-2 phase crystal structures (5):

$$\mathbf{c}_o = 0.55_s + 0.50\mathbf{b}_s + (3.38+0.27t)\mathbf{c}_s \qquad [13]$$

In the special case $t_2 = t_1 = 1/2t$, the methyl groups lie in a flat plane, so that the stacking of the layers is not governed by a terraced structure. A shift of the layers over $1/2\mathbf{a}$ ($=\mathbf{a}_s+1/2t\mathbf{c}_s$) can also be considered:

$$\mathbf{c} = \mathbf{c}_o + \mathbf{a}_s + 1/2\,(n+t)\,\mathbf{c}_s \qquad \text{for } t_2 = t_1 \qquad [14]$$

The long spacing can be easily evaluated as:

$$L = 1/2\,(n+n_o) \bullet c_s \bullet \sin\tau, \qquad [15]$$

where the value for n_o ($=6.76$) is virtually identical to the value for the β-2 phase (5).

(ii) In this case the **c** axis is unique, its length being equal to twice the long spacing. To a good approximation, the long spacing will not depend on the manner of layer stacking, i.e. Equation 15 applies quite generally.

The possible space groups are $P2_1/a$, $P2_1/b$, $P2_1/n$, $P2_1/m$. Calculations show that the $P2_1/m$ packing always involves too short (<0.155 nm) intermolecular atom-atom distances. Stacking the layers around a glide plane is only permitted for the (−1,2) and the (−2,2) terraces in the case of an *a*-glide, for the (0,1) and (0,0) terraces in the case of a *b*-glide and for the (0,1), (0,0) and (−1,1) terraces in the case of a diagonal glide.

(iii) The unique axis lies in the (001) plane and coincides with **a**, **b** or **a**+**b**. Since a unique axis has to be at right angles to the other unit-cell axes, we need to examine whether there is one pair of axes in the *ab*-plane which happens to meet this requirement. We verified that there is no such pair for $t=0$ or $t=1$, unless the γ_s angle is unduly altered. Therefore the possibility of a layer stacking around a twofold (screw) axis can be safely disregarded.

So the allowed space groups are: $P\bar{1}$, $P2_1/a$, $P2_1/b$ and $P2_1/n$. Unfortunately distinguishing between the various alternatives solely on the basis of powder diffraction data is impossible. In the next section we will further investigate this structural aspect by means of lattice-energy calculations.

Lattice-energy calculations—method of calculation. The lattice energy of a molecular crystal is assumed to be a pairwise additive sum of intermolecular interaction energies. In turn, these intermolecular energies are calculated as a pairwise sum of isotropic atom-atom interaction energies, which usually are composed of three terms: *(i)* a short-range repulsion term, $A\bullet\exp(-Br)$; *(ii)* a London-van der Waals attraction, $-Cr^{-6}$; and *(iii)* an electrostatic term, q_iq_j/r. The above procedure is known as the atom-atom potential method (26–28) and has been widely used, e.g. by Hageman and Rothfus for the analysis of fat crystal structures (29–31).

In our calculations, the empirical potential parameters *A*, *B* and *C* were taken for Reference 32 for C•••C and H•••H and from Reference 33 for O•••O interactions. For heteronuclear interactions, geometric averages for *A* and *C* and arithmetic averages for *B* were taken. The fractional atomic point charges, q_i, for the polar glycerol/ester fragment were taken from a *CNDO/2* molecular orbital calculation (34) which we carried out for triacetylglycerol; the H atoms in the neutral CH_3 and CH_2 groups were assigned a charge of +0.11 *e* (35). The geometry of the molecules was not varied in our calculations. These were carried out using the crystal-packing program *PCK6*, which evaluates the lattice energy according to the above concepts together with its first and second derivatives with respect to the structural variables. The program subsequently searches for an energy minimum employing a steepest descent and/or a modified Newton-Raphson technique. Further details about the general procedure and its implementation in the *PCK6* program can be found in the literature (36).

We have altered this program in a few respects. The most significant is the addition of estimates for truncation errors in the lattice-energy summation (37); these were not accounted for in the original version. Through this modification we not only obtain more accurate results, but also an estimate of the precision of the final results. Another useful alteration concerns the efficiency of the minimization process when the structure is removed far from the energy minimum and the potential-energy hypersurface does not have positive curvature in all directions. In such cases, a partial energy minimization along the eigenvector associated with the negative eigenvalue of the second-derivatives matrix proves to be very effective.

The starting crystal structures were generated by the *BETA2* program (5). The atomic coordinates of β-2 *10.10.10* (24) are first transformed to the $T_{/\!/}$ subcell space for which the origin has been taken in the center of symmetry near the "corner" in chain 3. In the subcell space, *10.10.10* is easily transformed into any triacylglycerol *p.q.r* by adding or deleting in each of the three acyl chains the appropriate number of CH_2 groups. Subsequently, the atomic coordinates are transformed back again to the unit-cell appropriate to the triacylglycerol and the sub-modification under consideration, using the relevant expressions given in Reference 5.

A reliable comparison requires triacylglycerols having the same total number of chain carbon atoms, $n=p+q+r$. To save computer time and to attain sufficient precision, low-molecular-weight compounds must be used. On the other hand, the typical long-chain characteristics in a homologous series only appear with chain lengths of more than about six carbon atoms. The triacylglycerols chosen for the computations, *8.8.12* and *10.8.10* ($n=28$), meet the requirements imposed by the above restrictions.

Lateral packing. The geometric packing analysis indicated two possibilities for the lateral packing, viz. an **a**-axis packing obeying Equation 2, with $t=+1$ or -1, the **b** axis given by Equation 8. This result, however, was based upon contact-distance criteria, and it was considered that a change in the molecular geometry might lower the potential energy. It would then be interesting to know the relative energies of the various lateral packing modes. We have, therefore, calculated the "lattice" energy of a single layer U_{layer}, for a wide range of *t* values.

The results are illustrated in Figure 5. The $t=-1$ and $t=1$ structures are very clearly favored. The intermediate structure, $t=0$, has a lattice energy which is about 40 kJ/mol higher. It is hardly conceivable that

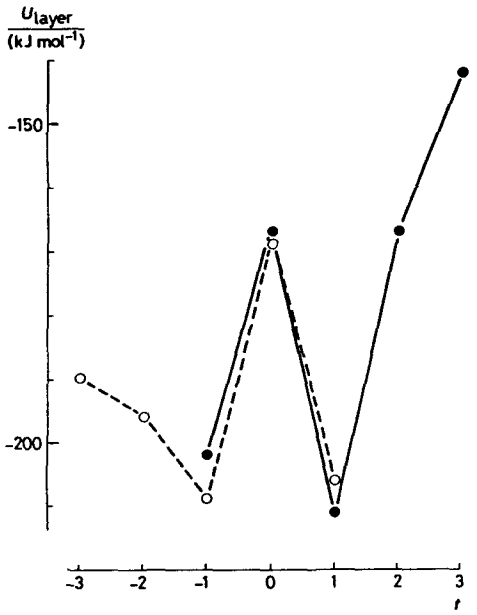

FIG. 5. Lattice energies [U_{layer}/(kJmol^{-1})] of saturated triacylglycerols in the β-3 phase for various lateral packings ($\mathbf{a}=2\mathbf{a}_s+t\mathbf{c}_s$; $\mathbf{b}=\mathbf{b}_s$). (●) *8.8.12;* (○) *10.8.10.*

such a large amount of energy can be absorbed by small adjustments of the molecular conformation. Thus, these lattice-energy calculations fully substantiate the earlier results of the simpler geometric analysis. The preference for the $t=-1$ or $+1$ packings can be traced back to the absence of a close contact between the carbonyl O of chain 3 and an H atom of either chain 1 ($t>1$), the glyceryl group ($t=0$) or chain 2 ($t<-1$) of a molecule translated over **a**+**b**. For the $t=-1$ or $t=+1$ structures, the O atom in question faces atoms which do not bear an H atom, i.e. the carbonyl C of chain 1 and the glycerol O connected to chain 2, respectively.

From now on we may confine our calculations to the $t=1$ packing mode, because the only other packing mode, viz. $t=0$, compatible with the experimental angle of tilt, has strongly repulsive lateral interactions.

Layer stacking. A second question concerning the β-3 phase crystal structures relates to the precise stacking of the layers (c-axis packing). Both for *8.8.12* and *10.8.10* we have calculated energy-minimized structures for each of the space-group symmetries under consideration, i.e. $P\bar{1}$, $P2_1/a$, $P2_1/b$, $P2_1/n$, and $P2_1/m$.

The results (Table 2) show that the two different methyl terraces lead to two distinct orders of increasing lattice energy, for the various layer-stacking modes, viz.:

$$P\bar{1} \approx P2_1/n << P2_1/b < P2_1/a < P2_1m$$
for *8.8.12* [(0,1) terrace] and

$$P\bar{1} \approx P2_1/a << P2_1/n < P2_1/b < P2_1/m$$
for 10.8.10 [(−1,2) terrace].

These results substantiate our earlier conclusions on this aspect of the β-3 crystal structures. Both for the (0,1) and the (−1,2) terrace, the second best structure differs only very little (ca. 1 kJ/mol) in energy from the "best" $P\bar{1}$ structure.

A subtle change of crystallization conditions may then yield crystals which differ only in the way the layers are stacked. An example of this type of polymorphism is provided by the longer, even alkanes such as $C_{36}H_{74}$ (38).

Table 2 also contains values for n_o. Here, we observe a perfect adherence to the close-packing principle (39): low-energy structures are associated with a closer packing at the methyl terrace. Further, our calculations predict a difference in long spacing of about 0.1 nm between the two methyl terraces. Such a difference is of the same order of magnitude as the experimental error in powder diffraction, but it should well show up in the more precise single-crystal data.

TABLE 2

Lattice Energies [U_{cryst}/(kJ mol^{-1})] and Long-Spacing Parameters (n_o) of β-3 Phase Triacylglycerols for Different Space Group Symmetries

Space group	*8.8.12*(β-3*A*)		*10.8.10*(β-3*B*)	
	U_{cryst}	n_o	U_{cryst}	n_o
$P\bar{1}$	−226.4	6.16	−220.4	7.04
$P2_1/n$	−225.1	6.29	−215.0	7.73
$P2_1/a$	−217.8	7.37	−219.8	7.06
$P2_1/b$	−220.0	7.00	−211.9	9.05
$P2_1/m$	−214.8	8.29	−208.5	10.30

EXPERIMENTAL

Long spacings. In Figure 6, the measured long spacings of β-3 triacylglycerols have been plotted as a function of n. It appears that the four groups of triacylglycerols, $r=p$, $p+2$, $p+4$ or $p+6$, are not distinct in regard to the long spacings. The least-squares linear equation for these experimental long spacings is:

$$L = (n+6.71)\cdot 0.116 \text{ nm}, \qquad [16]$$

which corresponds closely to the "theoretical" Equation 15 if $\tau=66.4°$. The standard errors in the parameter values are 0.57 and 0.0014 respectively; the residual standard deviation of L amounts to 0.045 nm. The experimental angle of tilt agrees very closely with a $t=0$ structure ($\tau=67.4°$) and rather closely with a $t=1$ structure ($\tau=70.0°$). Minor alterations of the subcell dimensions (e.g. $\alpha_s=69°$ and $\beta_s=108°$ instead of $\alpha_s=71°$ and $\beta_s=110°$) are sufficient to get perfect agreement for the $t=1$ structure. Such small changes in the subcell parameters are very well conceivable. An analysis of the $T_{//}$ subcell dimensions of about twenty crystal structures of long-chain compounds shows a variation (2σ) in the angles of about 4° (5).

Melting points. Also included in Figure 6 are the melting points. The triacylglycerols seem to fall into two classes: the triacylglycerols melting at high temperatures with $r=p$, $p+2$ or $p+4$ and the "low-melting" $p.q.p+6$ triacylglycerols. For a given n, the difference in the melting points for the two classes is about 5°C.

We previously showed that, for reasons of entropy, symmetric triacylglycerols ($p=r$) will melt at temperatures about 4–6°C higher than comparable triacylglycerols with essentially the same crystal structure (5). Besides, triacylglycerols having a common methyl terrace were also shown to fall on a common melting-point curve (after allowance for the symmetry effect). So, when we account for the symmetry, it turns out that the symmetric triacylglycerols $p.q.p$ are associated with the low-melting $p.q.p+6$ triacylglycerols, rather than with the high-melting $p.q.p+2$ and $p.q.p+4$ triacylglycerols.

This very state of affairs links entirely with the $t=1$ packing mode, because in that case the $p.q.p+2$ and $p.q.p+4$ triacylglycerols have the same (0,1)[=(1,0)] terrace and the $p.q.p$ and $p.q.p+6$ triacylglycerols have the (−1,2)[=(2,−1)] terrace. These terraces and the corresponding triacylglycerols will be designated as β-3*A* and β-3*B*, respectively. There is also qualitative agreement between the lattice energy calculations and the observed melting points: the *A* terrace has the lower lattice energy and corresponds to the higher melting-point curve.

Although the measured melting points support our proposed crystal structures with $t=1$, they do not exclude all other possibilities. However, solely on the basis of melting points, it can be shown that the $p.q.p+2$

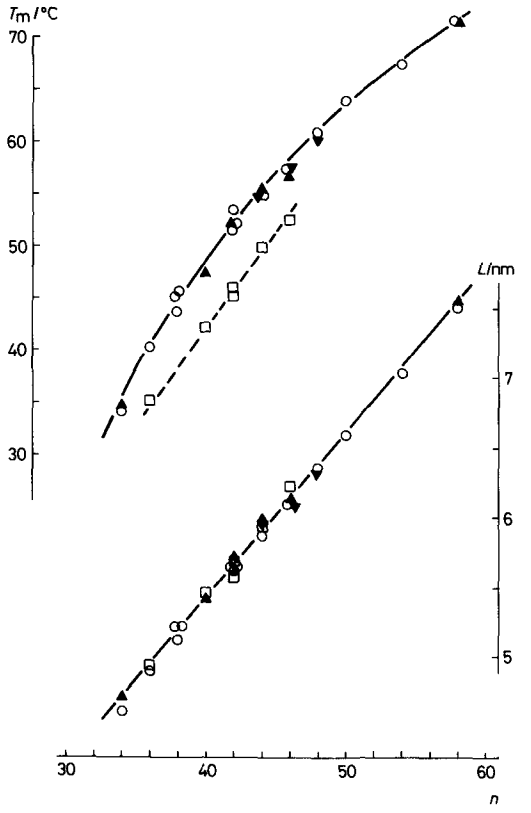

FIG. 6. Long spacings (L) and melting points (T_m) of saturated β-3 phase triacylglycerols as a function of the "total" chain length n. (○)$p.q.p$; (▼)$p.q.p+2$; (▲)$p.q.p+4$; (□)$p.q.p+6$.

triacylglycerols cannot adopt a $t=2$ structure [(0,2)-terrace]. In that case, one would also expect a $t=2$ structure [(2,0)-terrace] for $p.q.p+6$ triacylglycerols having comparable melting points for a given n, or even higher if there is a better structural alternative. In fact, we observe *lower* melting points for the $p.q.p+6$ series. Therefore, the starting assumption of a $t=2$ structure for $p.q.p+2$ triacylglycerols cannot be true. A similar comparison of $p.q.p+2$ to $p.q.p$ triacylglycerols demonstrates that the former do not adopt a $t=-1$ structure. Likewise, comparing $p.q.p+4$ to $p.q.p$ or to $p.q.p+6$ triacylglycerols excludes the $t=0$ and $t=3$ packing modes for $p.q.p+4$ triacylglycerols.

All in all, we may conclude that the observed melting points in combination with the results of the lattice-energy calculations strongly support the $t=1$ packing mode for all β-3 triacylglycerols.

Single-crystal data for 18.10.18. In 1968 Albon and Shipley succeeded in growing single crystals of β-3 *18.10.18* (unpublished results; cf. (1)). The unit-cell dimensions were determined to be $a=0.838$ nm, $b=0.5445$ nm, $c=11.71$ nm and $\gamma=114.6°$; space group $P2_1/a$. The short axes and the monoclinic angle are in good agreement with the values calculated for $t=1$: $a=0.824$ nm, $b=0.546$ nm and $\gamma=116.5°$ ($t=0$ would give $a=2a_s=0.876$ nm and $\gamma=\gamma_s=121°$). Our analysis of the various layer stackings also showed that $P2_1/a$ is a favorable space group for the β-3*B*-type terrace.

The length of the c axis, however, is problematic. The long spacing deduced from the single-crystal data ($L=1/2c=5.855$ nm) should agree with the long spacing obtained from powder diffraction [$L=6.12$ nm (7), or $L=6.14$ nm according to Equation 15 for $n=46$]. The difference of about 0.27 nm definitely exceeds any experimental uncertainties.

The unit-cell volume also points to an aberration. Interpolating between the unit-cell volumes of *14.14.14* ($n=42$, $Z=2$, $V=2.344$ nm^3, Reference 40) and *16.16.16* ($n=48$, $Z=2$, $V=2.619$ nm^3, Reference 41), one would predict a unit-cell volume of 5.054 nm^3 for *18.10.18* ($n=46$, $Z=4$). Albon and Shipley found 4.859 nm^3 (−3.9%), however. When the value $c=12.26$ nm ($=2L$) is used, the volume becomes 5.087 nm^3 (+0.6%). One would expect the β-3 phase to be less closely packed than the β-2 phase, rather than the other way around! The reported unit-cell data lead to a specific density, viz. 1.064 g/cm^3, that is exceptionally high compared to the range of 1.01-1.05 g/cm^3 observed for other β-phase triacylglycerols (1).

There remains the possibility that we are dealing with a new crystalline modification. This is not likely, however, unless it is accepted that the agreement for the other cell dimensions is fortuitous, and the laborious and difficult growth of a single crystal succeeded in the very case of a unique and peculiar β-3 modification.

We therefore are led to conclude that the reported length of the c axis is possibly in error by about 0.5 nm, probably because of the exceptional length of the c axis. Aside from this enigmatical c axis, we believe that the single-crystal data for *18.10.18* support our β-3*B* structure.

RESULTS AND DISCUSSION

Figure 7 shows a projection of the β-3*B* crystal structure of a $p.q.p$ triacylglycerol. As can be verified, a lengthening of chain 3 with six atoms to give a $p.q.p+6$ triacylglycerol does not affect the form of the methyl terrace. Likewise, Figure 8 shows the structure of a β-3*A* $p.q.p+4$ triacylglycerol. This structure may be compared with the $\beta=3A$ packing of $p.q.p+2$ shown in Figure 3.

The difference in melting points (about 5°C) between the *A*- and *B*-type triacylglycerols corresponds to about 3-4 kJ/mol difference between their melting enthalpies. The calculated lattice-energy difference (Table 2) is somewhat larger (5-6 kJ/mol), analogous to the situation for the β-2 phase triacylglycerols (37). Further, the calculated lattice-energy differences between the β-3 (Table 2) and the β-2 phase triacylglycerols (Ref. 37, Table 3.7) are somewhat higher than those derived from the melting-points. When considering all β-phase submodifications of saturated triacylglycerols, our calculations yield, for a given n, the following order of increasing lattice energy:

$$\beta\text{-}2D \approx \beta\text{-}2A < \beta\text{-}2C < \beta\text{-}2B \approx \beta\text{-}2E < \beta\text{-}3A < \beta\text{-}3B$$

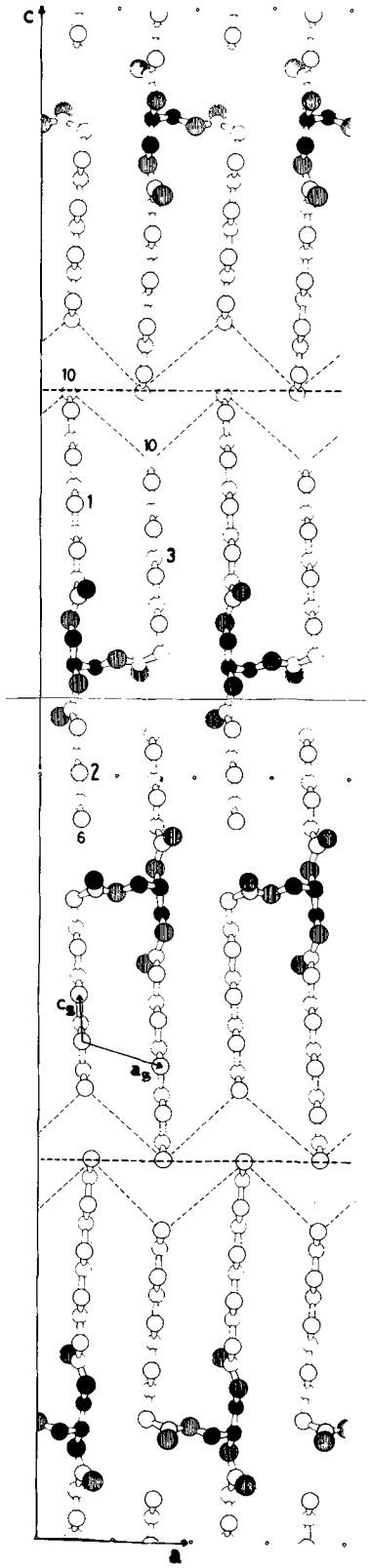

FIG. 7. Projection on (010) of the crystal structure of a *p.q.p* triacylglycerol (*10.6.10*) in the *β*-3*B* submodification. For the layer stacking we assumed an *a* glide (space group $P2_1/a$).

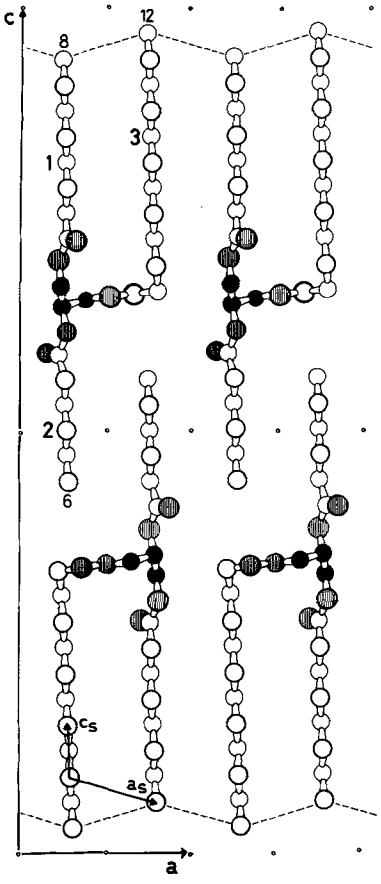

FIG. 8. Probable crystal structure of a *p.q.p*+4 triacylglycerol (*8.6.10*) in the *β*-3*A* submodification. $P\bar{1}$ symmetry assumed.

This conforms fully to the observed order of increasing melting point (after allowance has been made for the symmetry effect). It also shows clearly that the *β*-2 packing mode is preferred to the *β*-3 packing mode if a *β*-2 packing leads to an acceptable methyl terrace, i.e. if the middle chain is not exceptionally short or long.

The packing scheme put forward results in a detailed description of the crystal structures of four classes of saturated triacylglycerols crystallizing in two *β*-3 submodifications. As the lateral packing is the same for both submodifications ($\mathbf{a}=2\mathbf{a}_s+\mathbf{c}_s$), the difference lies only in the methyl terrace. The *β*-3*A* type triacylglycerols *p.q.p*+2 and *p.q.p*+4 have a smoother terrace than the *β*-3*B* type triacylglycerols *p.q.p* and *p.q.p*+6. In common with the *β*-2 phase triacylglycerols, the observed melting-point lines for the four classes of triacylglycerols can be understood on the basis of both structural and thermodynamic considerations. Much of the work presented here will be of use in the crystal packing analysis of unsaturated triacylglycerols, which will be discussed in a forthcoming paper.

REFERENCES

1. Shipley, G.G., in *The Physical Chemistry of Lipids (Handbook of Lipid Research, Vol. 4)*, edited by D.M. Small, Plenum Press, New York, New York, 1986, pp. 97–147.
2. Hernqvist, L., in *Crystallization and Polymorphism of Fats and Fatty Acids*, edited by N. Garti and K. Sato, Dekker, New York, New York, 1988, pp. 97–137.
3. Hagemann, J.W., *Ibid.*, pp. 9–95.
4. Timms, R.E., *Progr. Lipid Res. 23*:1 (1984).
5. de Jong, S., and T.C. van Soest, *Acta Crystallogr. B34*:1570 (1978).
6. Lutton, E.S., *J. Am. Chem. Soc. 70*:248 (1948).
7. Malkin, T., and M.L. Meara, *J. Chem. Soc.*, 1141 (1939).
8. Jackson, F.L., B.F. Daubert, C.G. King and H.E. Longenecker, *J. Am. Chem. Soc. 66*:289 (1944).
9. Jackson, F.L., R.L. Wille and E.S. Lutton, *Ibid. 73*:4280 (1951).
10. Gray, M.S., and N.V. Lovegren, *J. Am. Oil Chem. Soc. 55*:601 (1978).
11. Averill, H.P., J.N. Roche and C.G. King, *J. Am. Chem. Soc. 51*:866 (1929).
12. Lovegren, N.V., and M.S. Gray, *J. Am. Oil Chem. Soc. 55*:310 (1978).
13. Heiduschka, A., and H. Schuster, *J. Prakt. Chem. 120*:145 (1928).
14. Robinson, H.E., J.N. Roche and C.G. King, *J. Am. Chem. Soc. 54*:705 (1932).
15. Jackson, F.L., and E.S. Lutton, *Ibid. 71*:1976 (1949).
16. Jackson, F.L., and E.S. Lutton, *Ibid. 72*:4519 (1950).
17. Filer, L.J., S.S. Sidhu, C. Chen and B.F. Daubert, *Ibid. 67*:2085 (1945).
18. Perry, E.S., W.H. Weber and B.F. Daubert, *Ibid. 71*:3720 (1949).
19. Verkade, P.E., J. van der Lee and W. Meerburg, *Recl. Trav. Chim. Pays-Bas 56*:365 (1937).
20. Carter, M.G.R., and T. Malkin, *J. Chem. Soc.*, 1518 (1939).
21. Fischer, E., M. Bergmann and H. Bärwind, *Chem. Ber. 53*:1589 (1920).
22. Lutton, E.S., and A.J. Fehl, *J. Am. Oil Chem. Soc. 49*:336 (1972).
23. Chapman, D., *J. Chem. Soc.*, 3186 (1958).
24. Jensen, L.H., and A.J. Mabis, *Acta Crystallogr. 21*:770 (1966).
25. Vand, V., *Acta Crystallogr. 7*:697 (1954).
26. Kitaigorodsky, A.I., *Molecular Crystals and Molecules*, Academic Press, London, 1973.
27. Kitajgorodskij, A.I., in *Advances in Structure Research by Diffraction Methods*, edited by R. Brill and R. Mason, Wiley, New York, 1970, pp. 173–247.
28. Williams, D.E., and T.L. Starr, *Comput. Chem. 1*:173 (1977).
29. Hagemann, J.W., and J.A. Rothfus, *J. Am. Oil Chem. Soc. 60*:1123 (1983).
30. Hagemann, J.W., and J.A. Rothfus, *Ibid. 60*:1308 (1983).
31. Hagemann, J.W., and J.A. Rothfus, *Ibid. 65*:638 (1988).
32. Starr, T.L., and D.E. Williams, *Acta Crystallogr. A33*:771 (1977).
33. Kitaigorodskii, A.I., K.V. Mirskaya and V.V. Nauchitel', *Sov. Phys. Crystallogr. 14*:769 (1970).
34. Pople, J.A., and D.L. Beveridge, *Approximate Molecular Orbital Theory*, McGraw-Hill, New York, New York, 1970.
35. Warshel, A., and S. Lifson, *J. Chem. Phys. 53*:582 (1970).
36. Williams, D.E., *Acta Crystallogr. A28*:629 (1972).
37. de Jong, S., Triacylglycerol Crystal Structures and Fatty Acid Conformations. A Theoretical Approach, Thesis, State University Utrecht, The Netherlands, 1980.
38. Boistelle, R., B. Simon and G. Pèpe, *Acta Crystallogr. B32*:1240 (1976).
39. Kitaigorodskii, A.I., *Organic Chemical Crystallography*, Consultants Bureau, New York, 1957.
40. Precht, D., *Kiel. Milchwirtsch. Forschungsber. 29*:287 (1977).
41. Visser, J., *Joint Committee on Powder Diffraction Standards, Powder Diffraction File, Set 30*:1994 (1980).

[Received September 14, 1989; accepted March 7, 1990]